Phys. Status Solidi C **12**, No. 8, 1090–1093 (2015) / **DOI** 10.1002/pssc.201400249

physica status solidi c
www.pss-c.com
current topics in solid state physics

The photoresponse of crystalline silicon strained via ultrasonic cavitation processing

R. K. Savkina* **and A. B. Smirnov****

V. Lashkaryov Institute of Semiconductor Physics, NAS of Ukraine, pr. Nauki 41, 03028 Kiev, Ukraine

Received 22 September 2014, revised 12 July 2015, accepted 13 July 2015
Published online 28 July 2015

Keywords silicon, ultrasonic cavitation, surface photovoltage

* Corresponding author: e-mail r_savkina@lycos.com, Phone: +38 044 525 5461, Fax: +38 044 525 6296
** e-mail alex_tenet@isp.kiev.ua, Phone: +38 044 525 5461, Fax: +38 044 525 6296

(100)-oriented *p*-type silicon grown by the liquid-encapsulated Czochralski method was exposed to cavitation impacts to induce changes of the physical and structural properties of semiconductor. Optical and atomic force microscopy methods as well as X-ray diffraction, ellipsometry and photovoltage spectroscopy were used. By applying a high-intensity (15 W/cm^2) and high-frequency (1 ÷ 6 MHz) sonication technique we successfully formed a dendrite-like micron-scale array on a silicon surface. It was found also a surprising improvement in the photoelectric properties of silicon samples exposed to the megasonic processing. Significant rise in value and expansion of the spectral range of photosensitivity take place after cavitation treatment.

1 Introduction Cavitation impacts, which normally cause severe damage in hydraulic machinery, appear to be a promising and creative tool for chemistry and electronic engineering, as well as for medical/pharmaceutical and food industries [1-5]. Ultrasound (US) cavitation processing have found several applications in the last decade, such as cleaning and surface functionalizations, the development and optimization of new coatings, manipulation of surfaces at the atomic level. Extreme conditions of the ultrasonic cavitation such as local temperature and the pressure [6] are widely used in chemistry to synthesize nanomaterials [1], to enhance the electrochemical reactions and to modify the surface properties of electrodes [7], as well as to generate the novel materials in a liquid medium [8].

With respect to semiconductors, the main application of the acoustic cavitation is the ultrasonic cleaning. The behavior of semiconductor surfaces under the acoustic cavitation remains a little-studied. The possibility of the application of acoustic cavitation for material deposition from solution on semiconductor surface is confirmed by the results adduced in [9]. An original and environmentally friendly way to make Si surfaces porous by exposure to US cavitation processing in view of development of porous luminescent structures was described in [10]. It was also demonstrated the effectiveness of gettering by back-side damage introduced into a silicon wafer with a cavitating jet [11].

In the previous work, the suitable cavitation conditions to cause modification of the gallium arsenide surface up to the microscale pattern formation as well as in a change in the chemical composition of semiconductor have been successfully established [12, 13]. In this investigation, we use cavitations' impact to introducing mechanical stresses on silicon for its properties engineering.

2 Experiment Materials used in this study were boron-doped (100)-oriented p-type silicon wafers of diameter about 76.2-mm grown by the liquid-encapsulated Czochralski method. Samples were cut into 5 mm × 5 mm squares and were cleaned for 10 min in ethanol and then in ddH_2O (water for analytical laboratory use, ISO 3696:1987). All samples were treated by the cavitation impact in cryogenic liquid such as nitrogen (LN2).

For cavitation activation, a high frequency system (1 ÷ 6 MHz) with focused energy resonator described elsewhere [12] was used. Semiconductor target was placed inside the acoustically driven copper cell filled with technical liquid nitrogen, where the megasonic processing was initiated. The maximal value of the ultrasonic intensity was about

~ 15 W/cm^2 in the focus of the acoustic system. Post thermal annealing was carried out in the atmospheric ambient at 980 °C for 1 hour.

All processed surfaces were examined after fixed cavitation intervals using optical and atomic force microscopy. The structural characterization of the silicon samples was carried out by XRD in the standard symmetric reflection geometry using CuKα radiation. The optical characteristics of the typical annealed sample were studied by ellipsometry. All samples in the initial state and after the cavitation treatment were characterized by measuring their surface photovoltage spectra.

3 Results It was found that the sonication of the silicon samples has resulted in the essential change of the physical and structural properties of semiconductor surface. In particular, a significant rise of the photosensitivity occurs. As a measure of the photosensitivity we use the spectral distribution of the surface photovoltage. These measurements were performed using a lock-in detection scheme with modulation at 300 Hz at low level of homogeneous excitation by a monochromatic light in a wavelength range of λ = 0.5–2 μm.

3.1 Photovoltage spectra It was established that untreated Si samples exhibit very low level of the photovoltage response. The typical original photovoltage response obtained from samples investigated is shown in Fig. 1a. After sonication, significant rise in value of the photosensitivity as well as short-wavelength shift (0.11 eV) of its 'red' boundary from 1.158 eV to 1.265 eV was found. The annealing for the one hour at 980 °C resulted in the expansion of the spectral range of photovoltage response towards the visible region > 2 eV. Figure 1b illustrates surface photovoltage spectrum of the typical silicon sample after sonication and post thermal annealing. In order to determine positions of spectral components, we have used a deconvolution procedure with fitting to Lorentz functions. The photovoltage spectrum had complicated shape that could be described by a sum of three Lorentzian components. The energy positions of components were 1.07 eV, 1.15 eV, and 2.13 eV.

3.2 Surface morphology Additional investigations of the morphology of the surface of Si samples showed the following. AFM topographic measurements reveal that the initial surface was found to be totally flat, devoid of defects, with a measured roughness lower than 1 nm. The roughness was determined on a few randomly chosen areas of 40×40 μm^2. The cavitation-induced changes depended both on the processing duration and on the power and frequency of ultrasound. In contrast to kHz processing mode, the megasonic treatment does not lead to semiconductor surface degradation and fracture. All samples exhibited negligible surface modification up to at least the first 5 min. After about 10 min of testing time optical microscopy reveals small pits on the surface. Thereupon the character of surface modification becomes more complex. In particular, a dendrite-like micron-scale array formation inside the ultrasonically structured region at the maximum value of acoustic intensity in the LN was found. Microphotographs of the surface of samples after the cavitation treatment (Fig. 2a) clearly reveal characteristic regions formed under the action of the cavitating fluid. The results of AFM surface reconstruction showed that the structured surface occurs significantly below the initial surface level. Figure 2b illustrates the changes in the silicon surface after the post-sonication annealing.

3.3 Ellipsometry The optical characteristics of the typical annealed sample were studied by ellipsometry. The measurements were performed using a laser (λ = 632.8 nm) photoelectric compensation null ellipsometer (LEF 3G-1). The ellipsometric parameters Δ and ψ were determined from the results of multi-angle measurements in a range of incidence angle ϕ = 50°–75°. The ellipsometric data were interpreted and the optical parameters were calculated within the framework of the formation of the complex optical system with two transition layers

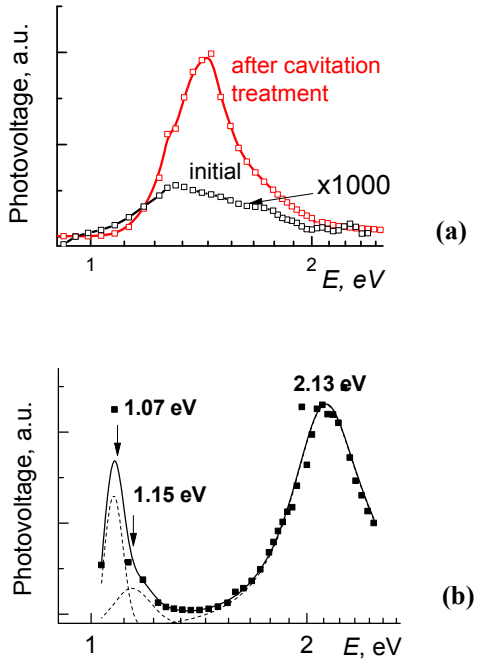

Figure 1 (a) Surface photovoltage spectra of the typical silicon sample exposured to the acoustic cavitation in liquid nitrogen at 3 MHz. The measured value of the photovoltage was about 30 μV at light power density ~0.01 W mm^{-2} after treatment. The solid lines are a guide to the eye. (b) The same sample after annealing of one hour's duration at 980 °C. The dots indicate the experimental data and the solid lines present the results of the fitting procedure. The thin dashed lines show approximation by the Lorentzian model.

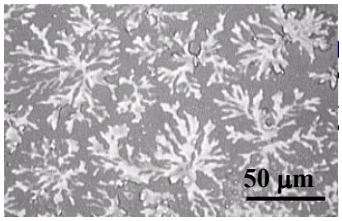

(a)

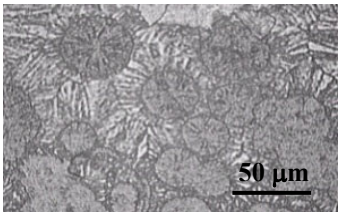

(b)

Figure 2 Optical micrographs of Si sample (a) exposed to the acoustic cavitation in liquid nitrogen at 3 MHz during 15 min; (b) the same sample after annealing of one hour's duration at 980 °C.

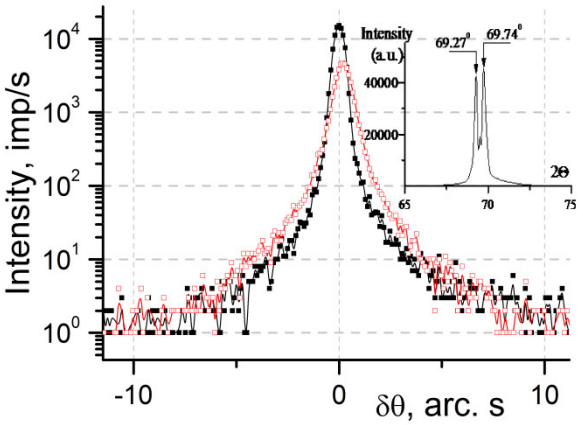

Figure 3 X-ray rocking curves for typical sample in initial state (■) and after cavitation treatment (□). Inset: Si(400) diffraction peak for sample after cavitation treatment.

after cavitation treatment and annealing. The values of the extinction coefficient k, the refractive index n and the thicknesses of layers are presented in the Table 1. The top (second) layer has optical parameters, which are close to SiO_2 compound. For precise definition of the first layer origin an additional research is required.

Table 1 Optical characteristics of a typical annealed silicon sample.

Layers	*n*	*k*	*d*
Substrate Si	3.88	0.029	Semi-infinity
First layer	3.12	0.026	500-900 nm
Second layer	1.43-1.48	$\rightarrow 0$	130 nm

3.4 X-ray diffraction The structural characterization of silicon samples was performed by XRD analysis in a classic reflection geometry using CuK_α radiation.

The initial XRD pattern reveal only the Si (400) diffraction peak that indicates on (100) orientation of the silicon wafer. XRD pattern obtained after cavitation treatment has more complex structure. It is need to note an essential increasing in the Si (400) diffraction peak intensity as well as splitting of this line (see inset Fig. 3). From the right of the intense peak at $2\theta = 69.27°$ corresponding to the reflection from the (400) plane of the silicon the intense peak at $2\theta = 69.74°$ was detected. Moreover, the peak with intensity $0.5I_{400}$ is observed between the mentioned peaks.

Using the strong (400) peak in the XRD pattern, the lattice parameters of the processed silicon is calculated to be a =5.4248 Å. These values are about 0.2% lower than the results for initial sample (a_o =5.4344 Å). Besides, the splitting of up to 0.01 Å (d-spacing) was detected for (400) peak.

It is well known that such change in XRD patterns as lines splitting as well as line broadening and shift can be connected with lattice strain. In our case, the upward shift of the silicon (400) peak, in comparison to the initial position of the one, points to a compressive strain in the semiconductor lattice after cavitation processing. It can be estimated as

$$\sigma = \frac{E\varepsilon}{(1-\nu)}, \quad (1)$$

$$\varepsilon = \Delta a / a_0, \quad (2)$$

where E is Young modulus, ν is Poisson's ratio. This gives a localized residual stress of ~1.55 GPa, which corresponds to a strain of about 1.19 %. The stress which causes the XRD peak splitting is mainly due to defect and chemical inhomogeneity in silicon after sonication. In particular, it can be related with the multilayer structure formation demonstrated by the ellipsometric data.

X-ray rocking curves (RC) for samples investigated before and after cavitation treatment were obtained using a Panalytical Xpert-pro triple-axis X-ray diffractometer from the symmetrical ω/2θ-scanning. X-rays were generated from copper linear fine-focus X-ray tube ($CuK_{\alpha 1}$ λ = 0.15418 nm). The initial RC has symmetric form. XRD results in the coherent-scattering region point out to the occurrence of the compressive strain in silicon samples after cavitation processing (Fig. 3).

4 Discussion Thus, the experimental study demonstrates that after the cavitation processing of the surface the formation of the microstructures array as well as significant rise of the photosensitivity occur. Besides, the XRD investigation pointed to stresses in the semiconductor lattice induced by the cavitation effect. The annealing for one hour at 980 °C resulted in the transformation of the photovoltage spectral distribution for samples processed. In addition, the formation of the complex optical system with

two transition layers after cavitation treatment and annealing takes place.

As a modulated illumination was used in our experiment, the surface photovoltage value can be expressed as [14]:

$$V_{PV}(\omega) = J_{PC}(\omega)\cdot Z_{eff}(\omega), \quad (3)$$

where the photocurrent density, J_{PC}, is typically extracted from a current-balance calculation and the effective impedance, Z_{eff}, is composed of parallel resistance (R_j) and capacitance (C_j) components, corresponding to the contributions of the various photovoltage influencing agents such as minority and majority carrier transport, depletion and inversion layers, surface states, etc.

In our case following factors could be indicated as influencing agents. First of all, a known phenomenon of the silicon wafer gettering by back-side damage introduced into a target with a cavitating jet [11] can result in the decrease in the rate of recombination through an energy state created within the band gap by a localized state. As a result the increases of carrier lifetime and diffusion length take place.

On the other hand, strains have been introduced into Si technology as a means of enhanced charge carrier mobility [15]. Applying advantageous strain modifies the band structure of Si in a way that the carrier mobility is increased through the reduction of its effective mass, and/or the suppression of scattering events to increase the relaxation time. It was shown that strain engineering for the CMOS applications are done at high temperature [16]. The treatment herein is based on a low-temperature approach by introducing compressive stress on silicon using US cavitation processing.

Finally, structuring of the surface is a known method to change the optical parameters and as a consequence to increase the efficiency of silicon solar cells. Flat silicon is fairly reflective even in the visible wavelength range. Such methods as anisotropic wet etching, reactive ion etching, laser processing are applied for silicon surface structurization. As a result, reducing the reflection of visible light increases the visible absorptance, making silicon surface more photosensitive. Thus, the photosensitivity rise of the silicon target can be connected *inter alia* with a dendrite-like micron-scale array formation on a silicon surface due to the cavitation processing.

According to the obtained results, we can see that the post-processing annealing of one hour's duration at 980 °C is an important factor of the expansion of the spectral range of silicon photosensitivity as well as formation of a multilayer optical system after cavitation treatment.

5 Conclusions Thus, it was found a surprising improvement in the photoelectric properties of silicon samples exposed to the US cavitation processing in the LN2. Significant rise in value and expansion of the spectral range of surface photovoltage take place after cavitation treatment. Crystalline silicon treated by the proposed method is characterized by expansion of the spectral interval of the photovoltage towards the visible region > 2 eV.

High-intensity sonication of silicon samples was shown to induce changes of the physical and structural properties of semiconductor surface. We successfully formed a dendrite-like micron-scale array inside ultrasonically structured region of Si. XRD results in the coherent-scattering region point out to the compression of the structured layer. Post-cavitation annealing of Si samples leads to the formation of a complex optical system with two transition layers with thickness from 0.6 μm to 1 μm. The photosensitivity rise of the silicon target can be connected with the surface micro-structurization, as well as ultrasound-induced lattice strain due to the cavitation processing of silicon.

Acknowledgements Authors are grateful to Dr.A.Gudymenko for XRD investigations.

References

[1] H. Xu, B. W. Zeiger, and K. S. Suslick, Chem. Soc. Rev. **42**, 2555 (2013).
[2] R. K. Savkina, Recent Patents on Electrical and Electronic Engineering **6**, 157 (2013).
[3] B. Kanegsberg and E. Kanegsberg (Eds.), Critical Cleaning Process Applications, Management, Safety, and Environmental Concerns (CRC Press, 2011).
[4] D. L. Miller, Prog. Biophys. Mol. Biol. **93,** 314 (2007).
[5] F. Chemat, Z. Huma, and M. K. Khan, Ultrason. Sonochem. **18**, 813 (2011).
[6] J. H. Bang and K. Suslick, Adv. Mater. **22**, 1039 (2010).
[7] M. Ashokkumar and T. Mason, Sonochemistry in Kirk-Othmer Encyclopedia of Chemical Technology (John Wiley and Sons, 2007).
[8] A. Gedanken, Ultrason. Sonochem. **11**, 47 (2004).
[9] S. Nomura and H. Toyota, Appl. Phys. Lett. **83**, 4503 (2003).
[10] E. V. Skorb, D. V. Andreeva, and H. Mçhwald, Angew. Chem. Int. Ed. **51**, 5138 (2012).
[11] H. Kumano, T. Sasaki, and H. Soyama, Appl. Phys**.** Lett. **85**, 3935 (2004).
[12] R. K. Savkina and A. B. Smirnov, J. Phys. D: Appl. Phys. **43**, 425301 (2010).
[13] R.K. Savkina and A. B. Smirnov, Tech. Phys. Lett. **41**, 164 (2015).
[14] L. Kronik and Y. Shapira, Surf. Sci. Rep. **37**, 1 (1999).
[15] F. Chen, Ch. Euaruksaku, Zh. Liu, F. J. Himpsel, F. Liu, and M. G. Lagally, J. Phys. D: Appl. Phys., **44,** 325107 (2011).
[16] B. Ghyselen, Mater. Sci. Eng. B **124-125**, 16 (2005).